A New Formula to Predict the Exact Detection Probability of a Generalized Order Statistics CFAR Detector for a Correlated Rayleigh Target

Chang-Joo Kim

CONTENTS

ABSTRACT

In this paper we present a new formula which can predict the exact detection probability of a generalized order statistics (GOS) constant false alarm rate (CFAR) detector for a partially correlated Rayleigh target model ($0 < \rho < 1$) in a closed form, where ρ is the correlation coefficient between returned pulses. By simply substituting a set of specific coefficient into the derived formula, one can obtain the detection probability of any kind of CFAR detector. Detectors may include the order statistics CFAR detector, the censored mean level detector, and the trimmed mean CFAR detector, but are not necessarily restricted to them. The numerical result for the first order Markov correlation model as applied to some of the detectors shows that as ρ increases from zero to one, higher signal-to-noise ratio is required to achieve the same detection probability.

I. INTRODUCTION

One of the most important problems in designing radar systems is the automatic detection of targets under varying environments. Since the background level is unknown and time-varying at any given location, the radar detector with a fixed threshold cannot be applied to the radar returns if one wants to control the false alarm rate. The *constant false alarm rate* (CFAR) detection technique is employed to control the false alarm rate, which estimates the background level and sets the threshold adaptively based on the local information of background level. The objective of the CFAR design is to provide detection threshold that is relatively immune to the varying background level and allow target detection with a CFAR.

Kanter [1] studied the detection performance of a noncoherent integration detector accumulating M correlated pulses from a Rayleigh target ($0 < \rho < 1$), but his work is limited only to radar detectors with fixed threshold. As mentioned above, radar detectors having fixed threshold cannot maintain CFAR. Kim *et al.* [2], [3] proposed and analyzed a CFAR detector based on *generalized order statistics* (GOS), which is known as the GOS CFAR detector. However, their work deals with target returns with completely correlated ($\rho = 1$) pulses or completely uncorrelated ($\rho = 0$) pulses.

In this paper, we extend the analysis of the GOS CFAR detector treated in [2], [3] to a correlated Rayleigh target model. As will be shown later, the GOS CFAR detector may be interpreted as a generalization of various other forms of *order statistics* (OS) CFAR detectors. By properly choosing its filter (GOS filter) coefficients, the GOS CFAR may become the OS CFAR detector [4], the *trimmed mean* (TM) CFAR detector [5], the *censored mean level detector* (CMLD) [6] or the *cell averaging* (CA) CFAR detector [7]. Thus, detection performances of these special case detectors for a correlated Rayleigh target model may be obtained by analyzing the GOS CFAR detector for the same target model, as shown in this paper.

This paper is organized as follows. Section II describes various target models considered in this paper. Section III derives expression for probabilities of detection and false alarm for a correlated Rayleigh target. Section IV presents analytical results and discussions. Conclusions are given in Section V.

II. TARGET MODEL DESCRIPTIONS

We introduce here some features of the Swerling target models as well as the correlated Rayleigh target model, which are essential in developing this paper.

1. Swerling Target Model

Swerling target models are well known for the radar detection [8]. They are based on four different models of target fluctuation and may be described by two different probability distributions with two different forms of fluctuation. When the target signal is constructed from many independently positioned scatterers, the resulting (received) signal on the radar cross section may be described by a Rayleigh distribution. Also, when the reflected signal contains a dominant constant component in addition to a Rayleigh distributed random component, the received signal can be described by a chi-square distribution with four degrees of freedom. As for the fluctuation, two cases are considered: scan-to-scan fluctuation and pulse-to-pulse fluctuation. The former assumes that the returned pulses in one scan are completely correlated ($\rho = 1$) and corresponds to Swerling I and III cases. The latter assumes that the returned pulses completely uncorrelated ($\rho = 0$) and thus corresponds to Swerling II and IV cases.

Equations we introduce in this section appeared previously in [1], [9]. To facilitate our discussion, we repeat them here (with our notations) with appropriate notes.

The chi-square family of distribution has been widely used to represent a fluctuating target. Let the signal-to-noise ratio (SNR) of a single pulse at the input to the detector be S, then the probability density function (pdf) of S may be written

$$p(S) = \frac{1}{\Gamma(K)}\left(\frac{K}{\overline{S}}\right)^K S^{K-1}\exp\left(-\frac{KS}{\overline{S}}\right), \quad S>0 \quad (1)$$

where $\overline{S}$ is the average of S, $K>0$ is a fluctuation parameter, representing the degree of freedom and $\Gamma(.)$ denotes the gamma function. $K = 1, M, 2, 2M$, and ∞ correspond to Swerling cases I, II, III, IV [8], and the nonfluctuation case, respectively.

The conditional moment generating function (mgf) of the statistic Y in Fig. 1 in the presence of a nonfluctuating target may be written

$$M_c(s|S) = (1+s)^{-M}\exp\left(-\frac{MS}{(1+s)}s\right). \quad (2)$$

The unconditional mgf for the chi-square family of fluctuating targets is then given by averaging (2) with respect to S using (1):

$$\begin{aligned} M_u(s) &= \int_0^\infty M(s|S)p(S)\,dS \\ &= \frac{(1+s)^{K-M}}{\left[1+s\left(1+\frac{M\overline{S}}{K}\right)\right]^K}. \end{aligned} \quad (3)$$

2. Correlated Rayleigh Target Model

The general formula of mgf for the Rayleigh target which is partially correlated from pulse to pulse is given [1] by

$$\begin{aligned} M_R(s) &= \frac{1}{(s+1)^M} \\ &\times\left[\int_{-\infty}^{\infty} p(\mathbf{A})\exp\left(-\frac{s}{s+1}\frac{|\mathbf{A}|^2}{2\sigma^2}\right)d\mathbf{A}\right]^2 \end{aligned} \quad (4)$$

where σ^2 is the variance of Gaussian noise involved in the definition of the Rayleigh target, $\mathbf{A}$ is the $M\times 1$ vector of the received signal amplitude, and $p(\mathbf{A})$ is the pdf of $\mathbf{A}$. For a correlated Rayleigh target, $p(\mathbf{A})$ is generally modeled as

$$p(\mathbf{A}) = \frac{\exp\left[-(1/2\bar{a}^2)\mathbf{A}^T\mathbf{R}^{-1}\mathbf{A}\right]}{(2\pi)^{M/2}|\bar{a}^2\mathbf{R}|^{1/2}} \quad (5)$$

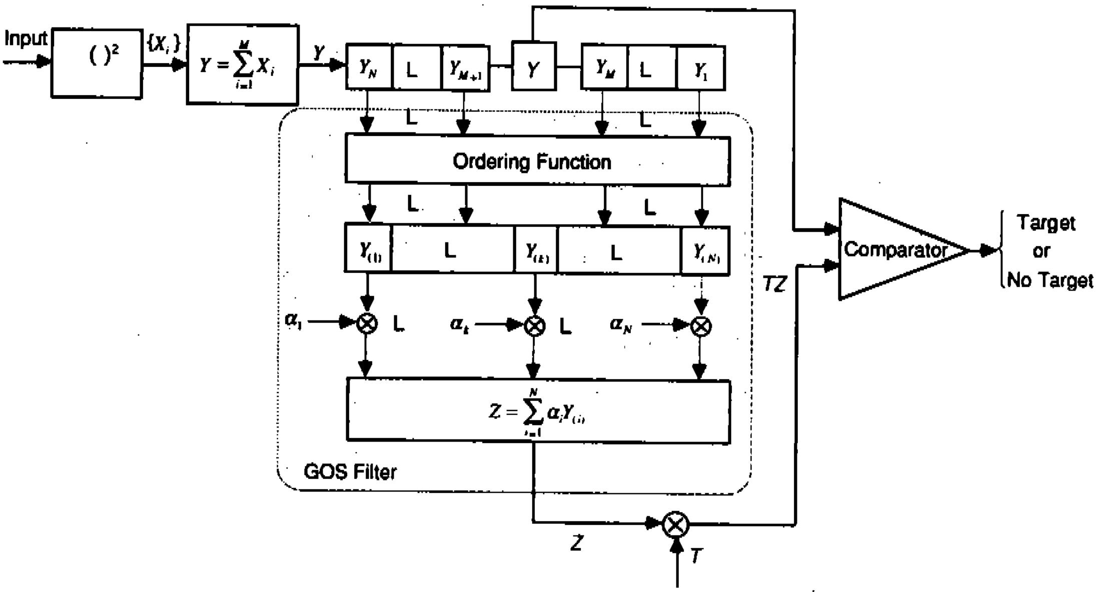

Fig. 1. Block diagram of the GOS CFAR detector with noncoherent integration.

where $\mathbf{R}$ is the correlation matrix of $\mathbf{A}$, superscript T denotes transpose, and $\bar{a}^2$ is the average target cross section, which is linearly related to the target power. With some manipulations, (4) becomes

$$M_R(s) = \frac{1}{(s+1)^M} \frac{1}{|\mathbf{R}|\,|\mathbf{R}^{-1}+[s/(s+1)]\bar{S}\mathbf{I}|} \times \left[\int_{-\infty}^{\infty} \frac{\exp\{-(1/2\bar{a}^2)}{(2\pi)^{M/2}} \frac{\mathbf{A}^T(\mathbf{R}^{-1}+[s/(s+1)]\bar{S}\mathbf{I})^{-1}\mathbf{A}\}}{|\bar{a}^2(\mathbf{R}^{-1}+[s/(s+1)]\bar{S}\mathbf{I})^{-1}|^{1/2}} d\mathbf{A} \right]^2 = \frac{1}{|(s+1)\mathbf{I}+s\bar{S}\mathbf{R}|} \tag{6}$$

where $\mathbf{I}$ is identity matrix and $\bar{S}=\bar{a}^2/\sigma^2$. Expressing the determinant in terms of nonnegative eigenvalues, (6) becomes [1]

$$M_R(s) = \frac{1}{\prod_{i=1}^{M}[(1+\lambda_i\bar{S})s+1]} \tag{7}$$

where λ_i's are the eigenvalues of the correlation matrix of target returns.

Swerling I and II cases can be obtained from (7) by choosing $\lambda_1 = M$ and $\lambda_i = 0$ $(i = 2, \ldots, M)$ for the slow fluctuation case $(\rho = 1)$ and $\lambda_i = 1$ $(i = 1, \ldots, M)$ for the fast fluctuation case $(\rho = 0)$

$$M_R(s)|_{\rho=1} = \frac{1}{(s+1)^{M-1}[(1+M\bar{S})s+1]} \tag{8}$$

and

$$M_R(s)|_{\rho=0} = \frac{1}{[(1+\bar{S})s+1]^M}, \tag{9}$$

respectively. Equations (8) and (9) can be also obtained from (3) with $K=1$ and with $K=M$, respectively.

III. GOS CFAR DETECTOR FOR A CORRELATED RAYLEIGH TARGET

Detection of a target in noise is achieved by hypothesis testing involving the null hypothesis H_0 (representing noise alone) and the alternative hypothesis H_1 (signal plus noise). The objective of the testing is to maximize the detection probability while limiting the probability of false alarm to a desired value. Decision is made in favor of H_1 or H_0 such that

$$Y \underset{H_0}{\overset{H_1}{\gtrless}} TZ \tag{10}$$

where Y is the test statistic of the cell under test, T is a threshold coefficient to achieve a desired false alarm probability for a given window size N, and Z is the estimate of the background level. Detection and false alarm probabilities, denoted as P_d and P_{fa}, respectively, may be written

$$P_d = \int_0^\infty f_Z(z) \int_{Tz}^\infty p_1(y)\, dy dz \tag{11}$$

and

$$P_{fa} = \int_0^\infty f_Z(z) \int_{Tz}^\infty p_0(y)\, dy dz, \tag{12}$$

where $p_j(y)$ $(j=0,1)$ is the pdf of the test statistic Y for the presence $(j=1)$ and the absence $(j=0)$ of a target, respectively, and $f_Z(z)$ is the pdf of the random variable Z, which is defined in (15). These two quantities may be expressed in terms of mgf [3], [9], [10]:

$$P_{fa} = -\sum_{k0} \mathrm{res}\left[M_0(s)\frac{M_Z(-Ts)}{s}, s_{k0}\right] \tag{13}$$

and

$$P_d = -\sum_{k1} \mathrm{res}\left[M_1(s)\frac{M_Z(-Ts)}{s}, s_{k1}\right] \tag{14}$$

where $M_j(s)$ $(j=0,1)$ is the mgf for $p_j(y)$, s_{k0} ($k0=1,2,\ldots$) and s_{k1} $(k1=1,2,\ldots)$ are the poles of $M_0(s)$ and $M_1(s)$ lying in the left half plane, respectively, $M_Z(-Ts)$ is obtained by replacing s by $-Ts$ in the mgf of the pdf $f_Z(z)$, and res[.] denotes the residue.

A block diagram of the GOS CFAR detector with noncoherent integration is shown in Fig. 1. The GOS CFAR processor first orders samples of range cells according to their magnitudes. Then it multiplies the ordered samples by a set of coefficients defined by the GOS filter and sums the results to form an estimate of the background noise level. The output Z of the GOS filter of window size N is then [2], [3]

$$Z = \sum_{i=1}^{N} \alpha_i Y_{(i)} \tag{15}$$

where $Y_{(i)}$ is the i-th smallest sample among the N samples, and α_i's, $i=1,2,\ldots,N$, are a set of constant weights that can be chosen properly for an application. This estimate is now multiplied by a threshold coefficient T to yield the adaptive threshold TZ. The output of the cell under test will be then compared with this threshold TZ.

The main purpose of this paper is to evaluate the detection performance of the GOS

CFAR detector structure shown in Fig. 1. Detection and false alarm probabilities of this detector will be obtained with the help of (1) through (14).

There may be $(2^N - 1)$ kinds of CFAR processors obtained by combinations of α_i, $i = 1, 2, \ldots, N$, in the GOS CFAR detector. To show the relationship between the GOS CFAR detector and other CFAR processors, we denote the GOS CFAR detector as $\text{GOS}(n_1, n_2, \ldots, n_i, \ldots)$ CFAR processor, where n_i represents the position of each coefficient of the GOS filter whose value is 1. For example, the OS(k) CFAR detector can be represented as the GOS(k) CFAR processor, the CA CFAR detector as the $\text{GOS}(1, 2, \ldots, N)$ CFAR processor, the $\text{TM}(T_1, T_2)$ CFAR detector as the $\text{GOS}(T_1 + 1, \ldots, N - T_2)$ CFAR processor, and $\text{CMLD}(T_2)$ as the $\text{GOS}(1, \ldots, N - T_2)$ CFAR processor. Here the trimming parameters T_1 and T_2 represent the number of cells to be trimmed from the lower and upper ends after sorting the reference window data, respectively. In this way, we can implement the GOS CFAR detectors ranging from GOS(1) to $\text{GOS}(1, 2, \ldots, N)$ CFAR processor. The GOS( ) CFAR processor does not exist because it means $Z = 0$.

If the background noise level is Rayleigh, the output of the squarer $X = X_i$ is exponentially distributed under H_0 as

$$f_X(x) = \begin{cases} \exp(-x), & x > 0 \\ 0, & \text{otherwise.} \end{cases} \qquad (16)$$

The sum of X_i, say $Y = \sum_{i=1}^{\beta} X_i$, is gamma distributed and given by

$$\begin{aligned} f_Y(y) &= \frac{y^{\beta-1}\exp(-y)}{\Gamma(\beta)} \\ &\equiv G(\beta, 1), \quad y \geq 0,\ \beta \geq 0 \end{aligned} \qquad (17)$$

where β is an integer representing the number of x_i's summed over. Note that noncoherent integration is done by summing M independent and identically distributed samples from the squarer so that the output of the integrator, Y, is gamma distributed with $\beta = M$, i.e.,

$$Y \sim G(M, 1). \qquad (18)$$

Let $\{Y_1, \ldots, Y_N\}$ be the N-dimensional vector in the reference window in Fig. 1, and $\{Y_{(1)}, \ldots, Y_{(N)}\}$ be the set of order statistics for $\{Y_1, \ldots, Y_N\}$. The transformation from $\{Y_1, \ldots, Y_N\}$ to $\{Y_{(1)}, \ldots, Y_{(N)}\}$ is not one-to-one. There is a total of $N!$ possible arrangements of $\{y_{(1)}, \ldots, y_{(N)}\}$ in increasing order of magnitude. Thus, there are $N!$ inverses to the transformation.

The mgf of the estimate of the background level is then obtained to be

$$\begin{aligned} M_Z(s) &= E_Z[\exp(-sZ)] \\ &= E_Y\left[\exp\left(-s\sum_{i=1}^{N} \alpha_i Y_{(i)}\right)\right] \\ &= \sum_{\text{all } N! \text{ inverses}} \\ &\int_0^{\infty} dy_{(1)} \frac{y_{(1)}^{M-1}\exp(-y_{(1)})}{\Gamma(M)} \times \cdots \\ &\times \int_{y_{(N-1)}}^{\infty} dy_{(N)} \frac{y_{(N)}^{M-1}\exp(-y_{(N)})}{\Gamma(M)} \\ &\times \exp\left(-s\sum_{i=1}^{N} \alpha_i y_{(i)}\right) \end{aligned}$$

$$= \sum_{\text{all } N! \text{ inverses}} \sum_{p_N=0}^{M-1} \sum_{p_{N-1}=0}^{M-1+p_N} \cdots \sum_{p_2=0}^{M-1+p_3} \prod_{i=1}^{N} \begin{pmatrix} M+p_i-1 \\ M-1 \end{pmatrix} \times \left(\sum_{j=i}^{N} (1+s\alpha_j) \right)^{-(M+p_{i+1}-p_i)} \quad (19)$$

where $p_{N+1} = p_1 = 0$ and all $N!$ inverses mean the possible transformations between $\{Y_1, \ldots, Y_N\}$ and $\{Y_{(1)}, \ldots, Y_{(N)}\}$.

Using (19) and (3) for (13), we obtain the false alarm probability for the Swerling target model

$$P_{fa} = \sum_{\text{all } N! \text{ inverses}} \sum_{p_N=0}^{M-1} \sum_{p_{N-1}=0}^{M-1+p_N} \cdots \sum_{p_2=0}^{M-1+p_3} \sum_{q_1=0}^{M-1} \sum_{q_2=0}^{q_1} \cdots \sum_{q_{N-T_2}=0}^{q_{N-T_2-1}} \times \prod_{i=1}^{N} \begin{pmatrix} M+p_{i+1}-p_i+q_i-q_{i+1}-1 \\ M+p_{i+1}-p_i-1 \end{pmatrix} \times \begin{pmatrix} M+p_i-1 \\ M-1 \end{pmatrix} \times \left(\frac{\left(T\sum_{j=i}^{N} \alpha_j \right)^{q_i-q_{i+1}}}{\left(\sum_{j=i}^{N} (1+T\alpha_j) \right)^{M+p_{i+1}-p_i+q_i-q_{i+1}}} \right) \quad (20)$$

where $q_{N-T_2+1} = \cdots = q_N = 0$. Equation (20) corresponds to (16) in [3] with $C = 0$, where C is the clutter-to-noise ratio. If we set the number of integration to one, i.e., $M = 1$, (20) becomes

$$P_{fa} = \sum_{\text{all } N! \text{ inverses}} \prod_{i=1}^{N} \left(\sum_{j=i}^{N} (1+T\alpha_j) \right)^{-1} \quad (21)$$

Equation (21) corresponds to (16) in [2] with $C = 0$.

The detection probability for the Swerling target model may be obtained for two different conditions: $1 \le K < M$ and $1 \le M \le K$. For the first condition, $1 \le K < M$, (3) has two poles. One of them is the $(M-K)$th order pole at $s = -1$ and the other is the Kth order pole at $s = -F$, where $F = 1/(1+M\overline{S}/K)$. In this case, the detection probability is given by

$$P_d = \sum_{\text{all } N! \text{ inverses}} \sum_{p_N=0}^{M-1} \sum_{P_{N-1}=0}^{M-1+p_N} \cdots \sum_{p_2=0}^{M-1+p_3} \sum_{m=0}^{M-K-1} \sum_{q_1=0}^{m} \sum_{q_2=0}^{q_1} \cdots \sum_{q_{N-T_2}=0}^{q_{N-T_2-1}} \begin{pmatrix} M-m-2 \\ K-1 \end{pmatrix} \frac{(-F)^K}{G^{M-m-1}} \times \prod_{i=1}^{N} \begin{pmatrix} M+P_i-1 \\ M-1 \end{pmatrix} \begin{pmatrix} M+P_{i+1}-P_i+q_i-q_{i+1}-1 \\ M+p_{i+1}-p_i-1 \end{pmatrix} \times \left(\frac{\left(T\sum_{j=i}^{N} \alpha_j \right)^{q_i-q_{i+1}}}{\left(\sum_{j=i}^{N} (1+T\alpha_j) \right)^{M+p_{i+1}-p_i+q_i-q_{i+1}}} \right)$$

$$+\sum_{\text{all } N! \text{ inverses}} \sum_{p_N=0}^{M-1} \sum_{P_{N-1}=0}^{M-1+p_N} \cdots \sum_{p_2=0}^{M-1+p_3} \sum_{p=0}^{K-1} \sum_{q_1=0}^{p} \sum_{q_2=0}^{q_1} \cdots \sum_{q_{N-T2}=0}^{q_{N-T2-1}} (-1)^{q_1} \frac{(-F)^{K+q_1-p-1}}{G^{M-p-1}} \binom{M-p-2}{M-K-1} \times \prod_{i=1}^{N} \binom{M+p_i-1}{M-1} \binom{M+p_{i+1}-p_i+q_i-q_{i+1}-1}{M+p_{i+1}-p_i-1} \times \left(\frac{\left(T\sum_{j=i}^{N}\alpha_j\right)^{q_i-q_{i+1}}}{\left(\sum_{j=i}^{N}(1+TF\alpha_j)\right)^{M+p_{i+1}-p_i+q_i-q_{i+1}}} \right) \tag{22}$$

where $G = 1 - F$.

For the second condition, $1 \le M \le K$, (3) has the Kth order pole at $s = -F$, and the detection probability is given by

$$P_d = \sum_{\text{all } N! \text{ inverses}} \sum_{P_N=0}^{M-1} \sum_{P_{N-1}=0}^{M-1+p_N} \cdots \sum_{p_2=0}^{M-1+p_3} \sum_{m=M-1}^{K-1} \sum_{q_1=0}^{m} \sum_{q_2=0}^{q_1} \cdots \sum_{q_{N-T2}=0}^{q_{N-T2-1}} \binom{K-M}{K-m-1} \frac{F^{K+q_1-m-1}}{G^{M-m-1}} \times \prod_{i=1}^{N} \binom{M+p_i-1}{M-1} \binom{M+p_{i+1}-p_i+q_i-q_{i+1}-1}{M+p_{i+1}-p_i-1} \times \left(\frac{\left(T\sum_{j=i}^{N}\alpha_j\right)^{q_i-q_{i+1}}}{\left(\sum_{j=i}^{N}(1+T\alpha_j)\right)^{M+p_{i+1}-q_i+q_i-q_{i+1}}} \right) \tag{23}$$

Equations (22) and (23) correspond to (22) and (23) in [3], respectively, but these equations are repeated here for a logical development.

For correlated Rayleigh target, the detection probability may be obtained from (7), (14) and (19):

$$P_d = \sum_{\text{all } N! \text{ inverses}} \sum_{P_N=0}^{M-1} \sum_{P_{N-1}=0}^{M-1+p_N} \cdots \sum_{p_2=0}^{M-1+p_3} \sum_{n=1}^{M} \frac{1}{\prod_{\substack{\ell=1\\ \ell\neq n}}^{M}\left[1-\frac{1+\overline{S}\lambda_\ell}{1+\overline{S}\lambda_n}\right]} \times \prod_{i=1}^{N} \binom{M+p_i-1}{M-1} \left(\frac{1}{\left(\sum_{j=i}^{N}\left(1+\frac{T\alpha_j}{1+\overline{S}\lambda_n}\right)\right)^{M+p_{i+1}-p_i}} \right) \tag{24}$$

The false alarm probability is the same for both Swerling and correlated target models because (7) is equivalent to (3) when $\overline{S} = 0$.

IV. ANALYTICAL RESULTS AND DISCUSSION

In order to obtain detection performance for partially correlated target returns, we must provide the computation of eigenvalues [e.g., λ_i of (7)] of the correlation matrix $\mathbf{R}$. We assume that a) the statistics of the target signal are stationary, and b) the target signal is described by a first-order Markov process. Under these assumptions, R is a Toeplitz and nonnegative definite matrix.

$$\mathbf{R}=\begin{bmatrix} 1 & \rho & \rho^2\cdots\rho^{M-1} \\ \rho & 1 & \rho\cdots\rho^{M-2} \\ \vdots & \vdots & \ddots \quad \vdots \\ \rho^{M-1} & \rho^{M-2} & \cdots \quad 1 \end{bmatrix},\ 0\leq\rho\leq1. \tag{25}$$

We use the detection probability expressions obtained in Section III to evaluate the detection performances of the various CFAR detectors. Parameters to implement various CFAR detectors using the unified formula for the GOS CFAR detector, (24), are given in Table 1.

Table 1. Threshold coefficients (T) and GOS filter coefficients (α_i) for implementing various CFAR detectors ($N=8$, $P_{fa}=10^{-6}$)

CFAR Detectors	Coefficients of GOS Filter	Threshold Coefficient(T)
	$\alpha_1 \cdots \alpha_8$	$M=3$
CA CFAR	11111111	1.1544
OS(6) CFAR	00000100	8.9057
TM(5,1) CFAR	00000110	3.7844
CMLD(1)	11111110	1.5888

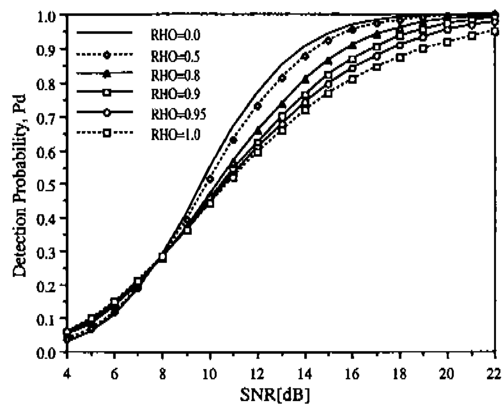

Fig. 2. Detection probabilities vs. target SNR for partially correlated Rayleigh target (CA CFAR detector).

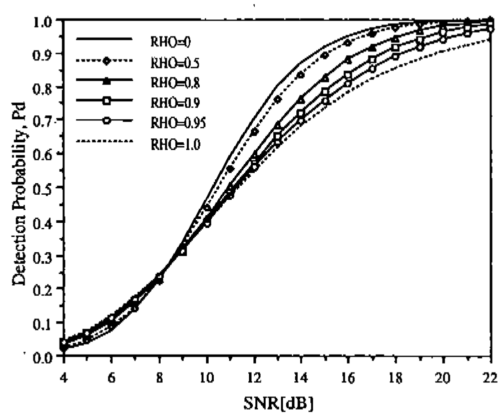

Fig. 3. Detection probabilities vs. target SNR for partially correlated Rayleigh target (OS CFAR detector).

Calculated performances of various CFAR detectors are shown in Figs. 2 - 5 as a function of per-pulse target SNR. Figs. 2 - 5 represent, respectively, the CA CFAR detector, the OS(6) CFAR detector, the TM(5,1) CFAR de-

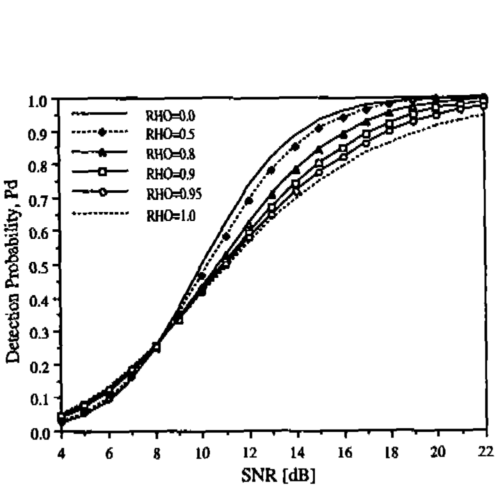

Fig. 4. Detection probabilities vs. target SNR for partially correlated Rayleigh target (TM CFAR detector).

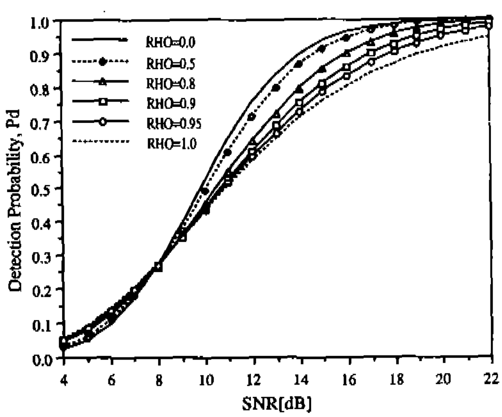

Fig. 5. Detection probabilities vs. target SNR for partially correlated Rayleigh target (CMLD(1) detector).

tector, and the CMLD(1). Note that $\rho = 0$ and $\rho = 1.0$ correspond to the Swerling I and II target models, respectively. These figures clearly show the effect of partial correlation (for $M = 3$ pulses). The solid curve with no symbol represents the Swerling II target ($\rho = 0$) and the dotted curve with no symbol represents the Swerling I target ($\rho = 1.0$). As seen, for $P_d > 0.27$, higher correlation means more fluctuation loss and requires higher (single pulse) SNR to achieve a given detection probability. When detection probability is low (e.g., $P_d \leq 0.27$), more fluctuation of target returns means some SNR gain; however, we are not interested in this low detection performance region. In order to reduce the effect of target fluctuation, one may employ pulse-to-pulse waveform diversity to decorrelate the returned signal pulse.

V. CONCLUSIONS

In this paper we have given an analysis of the GOS CFAR detector for a correlated Rayleigh target as well as four Swerling target models. The GOS CFAR detector may be interpreted as a generalization of various OS CFAR detectors, such as the OS CFAR, the TM CFAR, the CMLD, and the CA CFAR detectors. Detection probabilities for general correlation of target signals have been obtained in a closed form. By properly choosing filter coefficients (of the GOS CFAR detector), we can obtain the detection performance of each of these CFAR detectors. Detection performances were computed and plotted for the correlated Rayleigh target model as well as four Swerling target models.

It has been shown that target detectability is a function of correlation; detection probability decreases with increasing correlation. To improve detection performance, one may employ pulse-to-pulse waveform diversity and decorrelate the target returns.

REFERENCES

[1] I. Kanter, "Exact detection probability for partially correlated rayleigh targets," *IEEE Transactions on Aerospace and Electronic Systems*, AES-22, no. 2, pp. 184-196, Mar. 1986.

[2] C. J. Kim and H. S. Lee, "Analysis of the generalized OS CFAR detector," *ETRI Journal*, vol. 16, no. 1, pp. 17-34, Apr. 1994.

[3] C. J. Kim, D. S. Han, and H. S. Lee, "Generalized OS CFAR detector with noncoherent integration," *Signal Processing*, vol. 31, no. 1, pp. 43-56, Mar. 1993.

[4] H. Rohling, "Radar CFAR thresholding in clutter and multiple target situations," *IEEE Transactions on Aerospace and Electronics Systems*, AES-19, no. 4, pp. 608-621, July 1983.

[5] P. P. Gandhi and S. A. Kassam, "Analysis of CFAR processors in nonhomogeneous background," *IEEE Transactions on Aerospace and Electronics Systems*, AES-24, no. 4, pp. 427-445, July 1988.

[6] J. T. Rickard and G. M. Dillard, "Adaptive detection algorithms for multiple target situations," *IEEE Transactions on Aerospace and Electronics Systems*, AES-13, no. 4, pp. 338-343, July 1977.

[7] H. M. Finn and R. S. Johnson, "Adaptive detection mode with threshold control as a function of spatial sampled clutter level estimates," *RCA Review*, vol. 29, no. 3, pp. 414-464, Sept. 1968.

[8] P. Swerling, "Probability of detection for fluctuating targets," *IRE Transactions on Information Theory*, IT-6, no. 2, pp. 269-308, Apr. 1960.

[9] X. Y. Hou, N. Morinaga, and T. Namekawa, "Direct evaluation of radar detection probabilities," *IEEE Transactions on Aerospace and Electronic Systems*, AES-23, no. 4, pp. 418-424, July 1987.

[10] C. J. Kim and H. J. Lee, "Performance analysis of the clutter-map CFAR detector with noncoherent integration," *ETRI Journal*, vol. 15, no. 2, pp. 1-9, Oct. 1993.

Chang-Joo Kim was born in Kongju on December 21, 1956. He received the B.S. degree in electronics engineering from Hankuk-Aviation University in 1980, and the M.S. and Ph. D. degrees in electrical engineering from the Korea Advanced Institute of Science and Technology (KAIST) in 1988 and 1993, respectively. From 1980 to 1982 he was engaged as a research engineer at Agency for Defence Division (ADD). Since 1983 he has been with the communication fields of ETRI, where he is now senior research engineer of the Radio Signal Processing Section. His current interests include signal detection, channel coding, and digital signal processing.